PHYSICAL REVIEW B **71**, 121202(R) (2005)

Direct observation of a neutral Mn acceptor in $Ga_{1-x}Mn_xAs$ by resonant x-ray emission spectroscopy

Y. Ishiwata,[1,*] T. Takeuchi,[2] R. Eguchi,[1] M. Watanabe,[3] Y. Harada,[3] K. Kanai,[3] A. Chainani,[3] M. Taguchi,[3] S. Shin,[1,3] M. C. Debnath,[4] I. Souma,[4] Y. Oka,[4] T. Hayashi,[1] Y. Hashimoto,[1] S. Katsumoto,[1] and Y. Iye[1]

[1]*Institute for Solid State Physics, University of Tokyo, Kashiwanoha, Kashiwa, Chiba 277-8581, Japan*

[2]*Department of Applied Physics, Tokyo University of Science, Kagurazaka, Shinjyuku, Tokyo 162-8601, Japan*

[3]*RIKEN/SPring-8, Kouto, Mikazuki-cho, Sayo-gun, Hyogo 679-5143, Japan*

[4]*IMRAM, Tohoku University, Katahira, Aoba-ku, Sendai 980-8577, Japan*

(Received 21 May 2004; revised manuscript received 22 October 2004; published 16 March 2005)

We have investigated the Mn acceptor state of III-V-based diluted magnetic semiconductor $Ga_{1-x}Mn_xAs$ by means of high-resolution resonant x-ray emission spectroscopy, across the Mn L_3 edge. We identify the coexistence of signals related to the neutral impurity A^0 and the ionized acceptor state A^- in $Ga_{1-x}Mn_xAs$. This fact suggests that double-exchange-like interaction exists in the ferromagnetic coupling in addition to the free-carrier-induced interaction.

DOI: 10.1103/PhysRevB.71.121202 PACS number(s): 75.50.Pp, 75.30.Hx, 78.70.Ck, 78.70.En

The coexistence of localized and delocalized electrons in a doped system can lead to important properties for practical applications.[1–3] For example, hole doping in manganite perovskites create not only Mn-mixed valence but also ferromagnetism driven by the kinetics of Mn 3 *d* holes, based on the double-exchange (DE) interaction.[3] Heterovalent substitutions of magnetic impurities, as in diluted magnetic semiconductors (DMS) also introduce both magnetic moments and carriers that develop into carrier-induced ferromagnetism, a property whose origin is still under debate.[1,2] Carrier-induced ferromagnetism in III-V-based DMS $Ga_{1-x}Mn_xAs$ is especially important from the viewpoint of basic physics as well as application to devices due to comparatively high critical ferromagnetic temperature (T_c) and excellent connectivity to GaAs-based superstructures. In order to understand the carrier-induced ferromagnetism, it is essential to clarify the electronic state around a Mn acceptor. In the case that doping leads to dominantly ionized acceptor A^-, i.e., Mn^{2+} ion with a free hole, Rudermann-Kittel-Kasuya-Yoshida-like (RKKY-like) interaction is expected to give the appropriate explanation.[2,4] On the other hand, it follows from doping leading to neutral acceptor states A^0 being Mn^{3+} ion, or more appropriately, Mn^{2+} ion with a bound hole, that DE-like interaction should drive the ferromagnetism.[5] Previous high-energy spectroscopy reports on the Mn-partial-electronic state in $Ga_{1-x}Mn_xAs$ have mainly supported the A^- state.[6,7] On the other hand, electron paramagnetic resonance (EPR) of $Ga_{1-x}Mn_xAs$ has shown characteristic features due to coexistence of A^- centers along with A^0 centers for $x=0.0005$.[8] Further, infrared absorption spectroscopy of $Ga_{1-x}Mn_xAs$ with x close to the T_c maximum seems to support the formation of A^0 states because it has revealed highly localized character of carriers.[9]

Resonant x-ray emission spectroscopy (RXES) is an experimental technique that probes the emitted-photon energy (ω) of x rays under the excitation of a core electron near the absorption threshold.[10] The metal $2p \rightarrow 3d \rightarrow 2p$ RXES is a second-order (coherent absorption and emission of photons) optical process and hence *d-d* transitions are allowed, which are dipole forbidden for first-order optical processes. In the case of Mn $2p$ RXES for $Gn_{1-x}Mn_xAs$, since the on-site *d-d* transitions depend on the valency of Mn, it should be possible to resolve the structures of the A^0 (Mn^{3+} or Mn^{2+} with a bound hole; ^5D) state and the A^- (Mn^{2+}; ^6S) state clearly.[11] Note that the A^0 impurity of Mn^{2+} ion with a bound hole also has the same symmetry as a Mn^{3+} ion. For a metal impurity, one can observe wide-ranging *d-d* transitions due to the absence of strong overlapping interband transitions of the host material. Furthermore, the resonance effect should emphasize either the A^0 or A^- state by tuning incident-photon energy (Ω) to each absorption feature separated by the chemical shift.[12] Hence RXES is an important tool to characterize the Mn acceptor state in $Ga_{1-x}Mn_xAs$.

Recent work has shown the importance of interstitial Mn donors in $Ga_{1-x}Mn_xAs$ samples.[13–15] The interstitial Mn donors diffuse to the $Ga_{1-x}Mn_xAs$ surface upon annealing and form MnO, depending on temperature, in contrast to the immobile substitutional Mn acceptors.[16,17] Accordingly, one can identify the different Mn states upon annealing. RXES can be used for distinguishing between them due to the energy difference of the main peak in Mn L_3 ($2p_{3/2}$) region.[16] In this paper, we have performed high-resolution Mn L_3 RXES of as-grown and annealed $Ga_{0.953}Mn_{0.047}As$, $Cd_{0.78}Mn_{0.22}Te$, and Mn_2O_3. The study conclusively shows the presence of A^0 as well as A^- signals of $Ga_{1-x}Mn_xAs$.

$Ga_{1-x}Mn_xAs$ films were grown by molecular-beam epitaxy (MBE) on semi-insulating (001) GaAs substrates under As-rich conditions. This was followed by low-temperature (LT) annealing in a nitrogen gas environment for 15 min.[18] Substrate and annealing temperature were 230 and 260 °C. Temperature dependence of resistivity showed the metallic nature of as-grown and annealed films. The n_p was estimated from the Hall coefficient at room temperature (RT) and the T_c was determined from magnetization measurements. Details of the samples used in the present study are given in Table I. A $Cd_{1-x}Mn_xTe$ epilayer was also grown by MBE on (001)-oriented GaAs substrate. Mn_2O_3 was in powder form.

RXES and fluorescence yield (FY) measurements were performed at undulator beamline BL-2C in the photon factory of KEK.[19] The x-ray emission spectrometer uses a

TABLE I. The n_p (cm^{-3}) and T_c (K) for the samples of $Ga_{0.953}Mn_{0.047}As$.

Sample	n_p (cm^{-3})	T_c (K)
As-grown sample	5.9×10^{19}	55
LT-annealed sample	1.5×10^{20}	100

Rowland-circle geometry in which input slit, spherical grating, and multichannel detector lie on the focal circle.[20] The resolution of the beamline spectrometer was set to 0.3 eV. The total resolution of the RXES experiment was about 0.6 eV. The incidence angle was about 20° to the sample surface and the spectrometer was placed in the horizontal plane at an angle of 90° with respect to the incident beam. This configuration leads to a probe depth of more than 100 nm for L_3 emission of 3*d* transition metal ions.[21] No surface treatment was carried out prior to measurements. All measurements were performed at RT.

Figure 1(a) shows the x-ray absorption spectroscopy (XAS) spectra measured using an x-ray emission spectrometer and photo diode for as-grown (blue line) and LT-annealed (red line) $Ga_{0.953}Mn_{0.047}As$ in the Mn L_3 region, classified as the FY and the total photon yield (TPY) spectra, respectively. The TPY spectra are identical with the ones in previous work.[22] The FY spectra have a maximum intensity at the excitation energy Ω_1, while the TPY spectra exhibit a maximum at Ω_2. Further, the annealing dependence in FY is much smaller than that in TPY. The FY spectrum for the as-grown sample and the TPY spectrum for the LT-annealed sample well resemble the XAS (total electron yield) spectra after and before etching of Ref. 16, respectively. It has been shown that Mn interstitials diffuse towards the surface and form MnO upon LT annealing.[16,17] Therefore, the FY spectrum for the sample before annealing and the TPY spectrum after annealing should mainly reflect the bulk and surface Mn components, respectively. The differences in FY and TPY spectra are surprising as it indicates that FY is more bulk sensitive than TPY.

Figure 1(b) shows the RXES spectra plotted as a function of energy loss ω-Ω for as-grown (blue line) and LT-annealed (red line) $Ga_{0.953}Mn_{0.047}As$ in the Mn L_3 region. The RXES spectra 1–4 are normalized for incident-photon flux and measured time, and obtained with incident-photon energy Ω_{1-4} indicated in Fig. 1(a). The curve fittings using Gaussians for the RXES spectra of the as-grown sample clarify three features with intensities dependent on Ω and with constant energy loss compared to the elastic peak. The resonant inelastic x-ray scattering (RIXS) features are characteristic of *d*-*d* transitions rather than charge-transfer excitations, because they have narrow linewidths.[10] The spectrum 1 corresponds to bulk states and exhibits negligible annealing dependence. This shows that the RIXS features $I_{1,2}$ and N forming the spectrum 1 originate from the substitutional Mn acceptors insensitive to annealing.[17] The spectra 2 and 3 show small enhancements in intensity at equivalent loss energies of $I_{1,2}$ upon annealing. In particular, the spectrum 2 for the annealed sample probes the surface contribution as seen

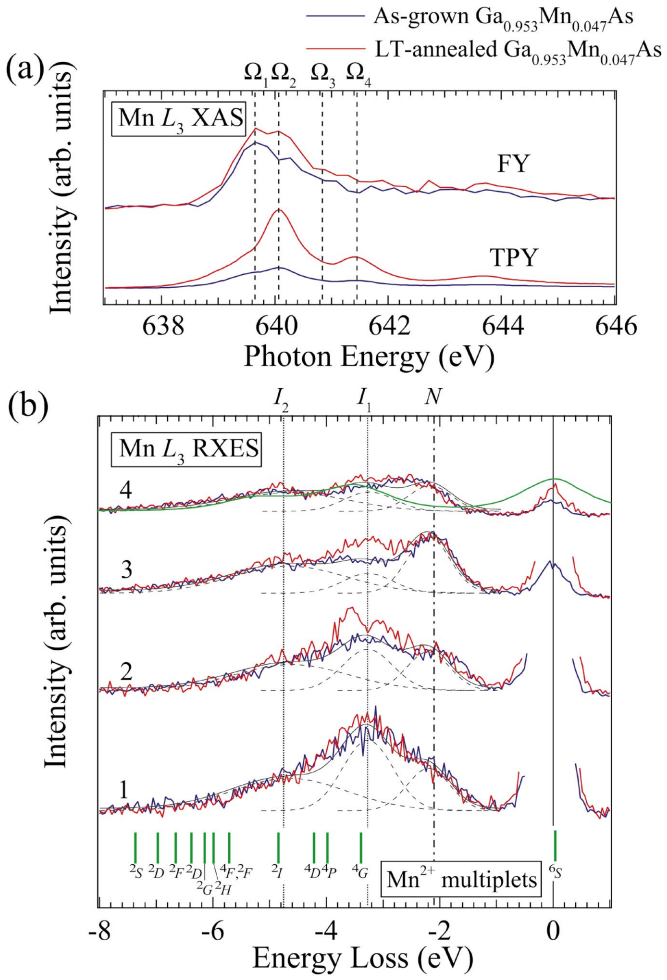

FIG. 1. (Color) (a) The XAS spectra measured using an x-ray emission spectrometer (FY) and photodiode (TPY) for as-grown (blue line) and LT-annealed (red line) $Ga_{0.953}Mn_{0.047}As$ in the Mn L_3 region at RT. The TPY spectra are identical with the ones in previous work (Ref. 22). (b) The RXES spectra plotted as a function of energy loss ω-Ω for as-grown (blue line) and LT-annealed (red line) $Ga_{0.953}Mn_{0.047}As$ in the Mn L_3 region at RT. The RXES spectra 1–4 were obtained with incident-photon energy Ω_{1-4} indicated in (a). Gaussian fittings for the RXES spectra of as-grown samples (black line) characterize three RIXS features, $I_{1,2}$, and N indicated by dotted and dash-dot lines, respectively. The RIXS calculation for a Mn^{2+} ion at the energy Ω_4 and Mn^{2+} atomic multiplets (green line and bar, respectively) are also shown (Refs. 23 and 24).

by the enhancement of a two-peak structure at loss energies of ~3.0 and 3.5 eV compared to that for the as-grown sample. Therefore, the increase in intensity in the spectra 2 and 3 upon annealing is attributed to surface MnO with more localized nature.[16] On the other hand, there is no RIXS feature decreasing in intensity upon annealing in Fig. 1(b); accordingly we cannot identify the feature corresponding to Mn interstitials. This is attributed to the low concentration of Mn interstitials. If Mn interstitials act as double donors,[13–15] the change in n_p by annealing suggests interstitial Mn donors are less than one-third of substitutional Mn acceptors in the as-grown sample (see Table I).

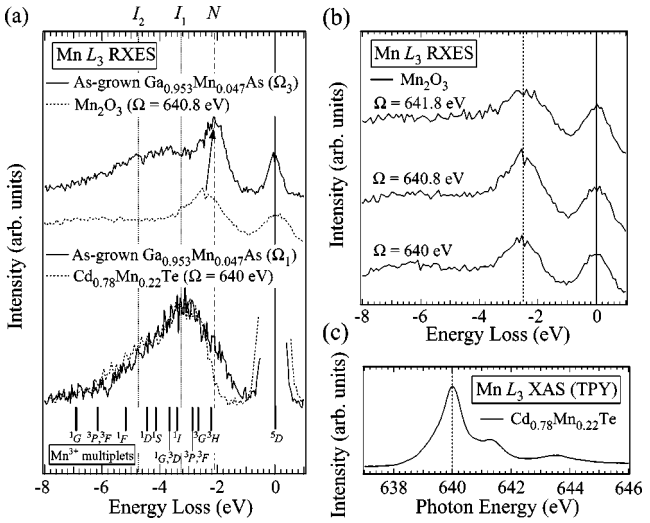

FIG. 2. (a) Two comparisons for the RXES spectra in the Mn L_3 region: (i) one between as-grown $Ga_{0.953}Mn_{0.047}As$ excited at Ω_1 (solid-line spectrum) and $Cd_{0.78}Mn_{0.22}Te$ excited at 640 eV (dashed-line spectrum) and (ii) the other between the as-grown $Ga_{0.953}Mn_{0.047}As$ excited at Ω_3 (solid-line spectrum) and Mn_2O_3 excited at 640.8 eV (dashed-line spectrum). The $Cd_{0.78}Mn_{0.22}Te$ and Mn_2O_3 spectra are scaled suitably for comparison. The Mn^{3+} atomic multiplets are shown as a bar diagram (Ref. 24). (b) The Mn_2O_3 RXES spectra at $\Omega = 640$, 640.8, and 641.8 eV. (c) The XAS (TPY) spectrum for $Cd_{0.78}Mn_{0.22}Te$ in the Mn L_3 region.

The RIXS features are divided into two groups named as $I_{1,2}$ (dotted line) and N (dash-dot line). The enhancement of $I_{1,2}$ mainly occurs at Ω_1 corresponding to the L_3 resonance of the FY spectrum for the as-grown sample with a line shape matching the cluster calculation for A^- (Mn^{2+}) excitations.[6] Further, the RIXS calculation for a Mn^{2+} ion at Ω_4 (green line) well reproduces $I_{1,2}$,[23] except for the slightly larger energy loss, which are probably due to the absence of cystal-field effects in the calculation.[11] This comparison suggests $I_{1,2}$ should be assigned to the *d-d* excitation originating from A^- (Mn^{2+}) states. Thus, we can attribute I_1 to ^4G, ^4P, and ^4D multiplet transitions and I_2 to ^2I, ^2F, and ^4F ones in a Mn^{2+} excitation,[23,24] as shown by the bar diagram in Fig. 1. On the other hand, N is enhanced at energy Ω_3 beyond the L_3 resonance. The difference between Ω_1 and Ω_3, corresponding to the resonance of $I_{1,2}$ and N, respectively, is about 1.3 eV and is comparable to the chemical shift between Mn^{2+} and Mn^{3+} states,[12] taking into account screening for A^- components.[16] The surface component related with the insulating MnO (Mn^{2+}) gives a resonance at Ω_2, lower than Ω_3 by about 0.8 eV.

The precise assignment of $I_{1,2}$ or N can be confirmed by comparison with the spectrum of reference samples containing Mn^{2+} or Mn^{3+} ions. As a reference to the A^- signal, we use II-VI-based DMS $Cd_{1-x}Mn_xTe$ in which a Mn impurity homovalently substitutes a Cd^{2+} ion.[1] Since there exists no DMS with a purely Mn^{3+} configuration, we use Mn_2O_3 as a reference of the A^0 signal. Basic properties of electronic states of $Ga_{1-x}Mn_xAs$ (Refs. 6 and 7) are almost the same as those of $Cd_{1-x}Mn_xTe$ (Ref. 25) and somewhat different from those of Mn_2O_3,[26,27] influencing *d-d* transitions. Figure 2(a) shows two comparisons for the RXES spectra in the Mn L_3 region: (i) one between as-grown $Ga_{0.953}Mn_{0.047}As$ excited at Ω_1 (solid-line spectrum) and $Cd_{0.78}Mn_{0.22}Te$ excited at 640 eV (dashed-line spectrum) and (ii) the other between the as-grown $Ga_{0.953}Mn_{0.047}As$ excited at Ω_3 (solid-line spectrum) and Mn_2O_3 excited at 640.8 eV (dashed-line spectrum). The $Cd_{0.78}Mn_{0.22}Te$ and Mn_2O_3 spectra are suitably scaled for comparison. The $Cd_{0.78}Mn_{0.22}Te$ measurement uses the excitation energy Ω corresponding to the photon energy at the L_3 absorption peak as shown in Fig. 2(c). The spectrum well reproduces $I_{1,2}$ and does not have any clear feature about N. On the other hand, the Mn_2O_3 spectrum at $\sim\Omega_3$ shows a RIXS feature near N, confirmed from constant energy loss irrespective of Ω as shown in Fig. 2(b). The RIXS feature also shows a similar enhancement at $\sim\Omega_3$ giving the resonance of N. The feature N matches with Mn^{3+} atomic multiplets [shown as bar diagram in Fig. 2(a)], with high-lying states overlapping Mn^{2+} states.[24] The *d-d* transitions of Mn^{3+} of trivalent $LuMnO_3$ also show a broad dominant feature (1.6–3.0 eV) and very weak features at higher energies.[28] The lower energy of the lowest *d-d* excitation of Mn^{3+} compared to Mn^{2+} is known to be due to smaller exchange stabilization compared to half-filled Mn^{2+} state.[11,24] Therefore it is concluded that $I_{1,2}$ and N correspond to the A^- and A^0 signals of $Ga_{1-x}Mn_xAs$. It is noted that the dominance of the A^- signals is not contradictory with the EPR and photoemission results.[6,8]

The coexistence of A^- and A^0 centers in $Ga_{1-x}Mn_xAs$ suggests consistency with a two-fluid model applicable to DMS in the vicinity of the metal-insulator transition in the presence of disorder, consisting of extended states and singly occupied impurity states, i.e., bound magnetic polarons (BMP).[29] It has been pointed out that the holes in the extended states mediate the long-range interactions between the localized spins and that the BMP makes ferromagnetic coupling with the neighboring A^- centers on the basis of DE-like interaction.[29] $Ga_{1-x}Mn_xAs$ samples used in this study are metallic even before annealing. This suggests the magnitude of spontaneous magnetization will attain $\sim$100%,[30] leading to the contribution of both A^- and A^0 centers to ferromagnetism. The two-fluid model is also consistent with the transport and magnetic measurements on the samples used in the present study.[31]

DE-like interaction causes fluctuation between A^0 and A^- centers in $Ga_{1-x}Mn_xAs$. The clear distinction in the RXES measurements is possibly due to the short lifetime of a Mn $2p$ hole.[32] On the other hand, EPR measurements have observed the A^0 signal only for very diluted GaAs:Mn, but not for $0.002 \leqslant x \leqslant 0.008$.[8] The delocalization accompanying the DE-like interaction possibly leads to a decoherence in active Mn acceptors, leading to a suppression of the EPR signal.

n_p or T_c of $Ga_{1-x}Mn_xAs$ samples depend on the Mn concentration as well as on the annealing procedure.[2,18] In our previous study,[22] we have found that the $Ga_{1-x}Mn_xAs$ TPY spectral intensity scaled with n_p or T_c. The TPY spectral intensity mainly reflects the surface MnO. Since the formation of surface MnO corresponds to the annihilation of interstitial Mn donors, it contributes to the increase of n_p and hence T_c in the system. Hence, n_p or T_c is determined by the

diffusion coefficient of interstitial Mn donors, which depends on the Mn concentration, substrate temperature, and the annealing temperature after growth.

In conclusion, we have studied the Mn acceptor state of III-V-based DMS $Ga_{1-x}Mn_xAs$ by high-resolution Mn L_3 RXES. By comparing with $Cd_{1-x}Mn_xTe$ and Mn_2O_3, we identify coexistence of major A^- signals and minor A^0 signals in $Ga_{1-x}Mn_xAs$. This suggests the existence of ferromagnetic coupling based on a DE-like interaction in addition to the free-carrier-induced interaction.

We would like to thank A. Kotani, T. Uozumi, M. Matsubara, and K. Kobayashi for meaningful advice, and A. Yagishita for technical support. This work was partly supported by a Grant-in-Aid for the Scientific Research from the Ministry of Education, Science, Sports, and Culture, Japan.

*Present address: Advanced Device Laboratory, The Institute of Physical and Chemical Research (RIKEN), 2-1 Hirosawa, Wako, Saitama 351-0198, Japan.

[1] J. K. Furdyna, J. Appl. Phys. **64**, R29 (1988), and references therein.

[2] H. Ohno, J. Magn. Magn. Mater. **200**, 110 (1999); H. Ohno, Science **281**, 951 (1998).

[3] A. Urushibara, Y. Moritomo, T. Arima, A. Asamitsu, G. Kido, and Y. Tokura, Phys. Rev. B **51**, 14 103 (1995), and references therein.

[4] F. Matsukura, H. Ohno, A. Shen, and Y. Sugawara, Phys. Rev. B **57**, R2037 (1998).

[5] H. Akai, Phys. Rev. Lett. **81**, 3002 (1998).

[6] O. Rader, C. Pampuch, A. M. Shikin, W. Gudat, J. Okabayashi, T. Mizokawa, A. Fujimori, T. Hayashi, M. Tanaka, A. Tanaka, and A. Kimura, Phys. Rev. B **69**, 075202 (2004).

[7] J. Okabayashi, A. Kimura, O. Rader, T. Mizokawa, A. Fujimori, T. Hayashi, and M. Tanaka, Phys. Rev. B **58**, R4211 (1998); J. Okabayashi, A. Kimura, T. Mizokawa, A. Fujimori, T. Hayashi, and M. Tanaka, Phys. Rev. B **59**, R2486 (1999).

[8] J. Szczytko, A. Twardowski, K. Świątek, M. Palczewska, M. Tanaka, T. Hayashi, and K. Ando, Phys. Rev. B **60**, 8304 (1999).

[9] K. Hirakawa, S. Katsumoto, T. Hayashi, Y. Hashimoto, and Y. Iye, Phys. Rev. B **65**, 193312 (2002).

[10] A. Kotani and S. Shin, Rev. Mod. Phys. **73**, 203 (2001).

[11] S. Sugano, Y. Tanabe, and H. Kamimura, *Multiplets of Transition Metal Ions in Crystals* (Academic, New York, 1970).

[12] H. Kurata and C. Colliex, Phys. Rev. B **48**, 2102 (1993).

[13] J. Blinowski and P. Kacman, Phys. Rev. B **67**, 121204(R) (2003).

[14] F. Máca and J. Mašek, Phys. Rev. B **65**, 235209 (2002).

[15] K. M. Yu, W. Walukiewicz, T. Wojtowicz, I. Kuryliszyn, X. Liu, Y. Sasaki, and J. K. Furdyna, Phys. Rev. B **65**, 201303(R) (2002).

[16] K. W. Edmonds, N. R. S. Farley, R. P. Campion, C. T. Foxon, B. L. Gallagher, T. K. Johal, G. van der Laan, M. MacKenzie, J. N. Chapman, and E. Arenholz, Appl. Phys. Lett. **84**, 4065 (2004); K. W. Edmonds, N. R. S. Farley, T. K. Johal, R. P. Campion, B. L. Gallagher, C. T. Foxon, and G. van der Laan, J. Appl. Phys. **95**, 7166 (2004).

[17] K. W. Edmonds, P. Bogusławski, K. Y. Wang, R. P. Campion, S. N. Novikov, N. R. S. Farley, B. L. Gallagher, C. T. Foxon, M. Sawicki, T. Dietl, M. B. Nardelli, and J. Bernholc, Phys. Rev. Lett. **92**, 037201 (2004).

[18] T. Hayashi, Y. Hashimoto, S. Katsumoto, and Y. Iye, Appl. Phys. Lett. **78**, 1691 (2001).

[19] M. Watanabe, A. Toyoshima, Y. Azuma, T. Hayashi, Y. Yan, and A. Yagishita, Proc. SPIE **58**, 3150 (1997).

[20] Y. Harada, H. Ishii, M. Fujisawa, Y. Tezuka, S. Shin, M. Watanabe, Y. Kitajima, and A. Yagishita, J. Synchrotron Radiat. **5**, 1013 (1998).

[21] J. Guo, P. Skytt, J. Wassdahl, and J. Nordgren, J. Electron Spectrosc. Relat. Phenom. **110-111**, 41 (2000).

[22] Y. Ishiwata, M. Watanabe, R. Eguchi, T. Takeuchi, Y. Harada, A. Chainani, S. Shin, T. Hayashi, Y. Hashimoto, S. Katsumoto, and Y. Iye, Phys. Rev. B **65**, 233201 (2002).

[23] S. M. Butorin, J.-H. Guo, M. Magnuson, P. Kuiper, and J. Nordgren, Phys. Rev. B **54**, 4405 (1996).

[24] D. van der Marel, C. Westra, G. A. Sawatzky, and F. U. Hillebrecht, Phys. Rev. B **31**, 1936 (1985).

[25] T. Mizokawa and A. Fujimori, Phys. Rev. B **48**, 14150 (1993).

[26] T. Uozumi, K. Okada, A. Kotani, R. Zimmermann, P. Steiner, S. Hüfner, Y. Tezuka, and S. Shin, J. Electron Spectrosc. Relat. Phenom. **83**, 9 (1997).

[27] J. Kawai, Y. Mizutani, T. Sugimura, M. Sai, T. Higuchi, Y. Harada, Y. Ishiwata, A. Fukushima, M. Fujisawa, M. Watanabe, K. Maeda, S. Shin, and Y. Gohshi, Spectrochim. Acta, Part B **55**, 1385 (2000), and references therein.

[28] A. B. Souchkov, J. R. Simpson, M. Quijada, H. Ishibashi, N. Hur, J. S. Ahn, S. W. Cheong, A. J. Millis, and H. D. Drew, Phys. Rev. Lett. **91**, 027203 (2003).

[29] T. Dietl, H. Ohno, F. Matsukura, J. Cibert, and D. Ferrand, Science **287**, 1019 (2000); T. Dietl, H. Ohno, and F. Matsukura, Phys. Rev. B **63**, 195205 (2001), and references therein.

[30] A. Oiwa, S. Katsumoto, A. Endo, M. Hirasawa, Y. Iye, H. Ohno, F. Matsukura, A. Shen, and Y. Sugawara, Solid State Commun. **103**, 209 (1997).

[31] S. Katsumoto, T. Hayashi, Y. Hashimoto, Y. Iye, Y. Ishiwata, M. Watanabe, R. Eguchi, T. Takeuchi, Y. Harada, S. Shin, and K. Hirakawa, Mater. Sci. Eng., B **84**, 88 (2001).

[32] M. O. Krause, J. Phys. Chem. Ref. Data **8**, 307 (1979).